Submitted to small

DOI: 10.1002/smll.201202710

Oxidation Level Dependent Zwitterionic Liposome Adsorption and Rupture by Graphene-based Materials and Light Induced Content Release **

*Alexander C-F. Ip, Biwu Liu, Po-Jung Jimmy Huang and Juewen Liu **

[*] Prof. J. L. Corresponding-Author
Department of Chemistry, Waterloo Institute for Nanotechnology, University of Waterloo, 200 University Avenue West, Waterloo, Ontario, N2L 3G1, Canada
E-mail: liujw@uwaterloo.ca

Supporting Information is available on the WWW under http://www.small-journal.com or from the author.

Keywords: graphene, liposomes, adsorption, controlled release, cryo-TEM

Graphene is a single layer of graphite with unique electrical, thermal, and optical properties and a large surface area; many novel materials and devices have been prepared using these properties.[1-7] To disperse in water, graphene oxide (GO) with surface hydroxyl, epoxy, and carboxyl groups is often used. One of the new research directions is to interface graphene and GO with biological systems, with examples including GO-based drug delivery vehicles,[8-10] biosensors,[11-15] imaging agents,[8, 16] and graphene-containing devices that can probe cells.[17] To further improve such materials and devices, one of the most fundamental questions is the interaction between lipid bilayers and graphene-based materials.[18-22]

Liposomes are often used to mimic the cell membrane.[23-26] Using supported lipid bilayers, cationic lipids have been shown to adsorb negatively charged GO, while no adsorption was observed with supported anionic membranes, which can be explained based on electrostatic interactions.[19] In an earlier study, various liposomes were interfaced with graphene deposited on a wafer for device fabrication.[18] The authors determined the diffusion coefficient of the PC membrane on graphene to be comparable with that on a glass surface, which puzzled the authors because of the hydrophobic nature of graphene. A trapped water layer was then suggested to bridge the lipid and the graphene surface. Finally, molecular dynamics simulation showed the insertion of a graphene sheet between the hydrophobic tails of a bilayer, which is equivalent to supported monolayers.[20]

With these progresses, many important questions remain to be answered. First, in previous work, either graphene was deposited on a wafer or the lipid bilayer was supported on a surface. We reason that colloidal graphene and liposomes are more likely to be used for biomedical applications. Second, it is unclear whether there are non-electrostatic intermolecular forces that allow liposomes, especially zwitterionic liposomes, to interact with GO. It is important to avoid cationic liposomes to minimize toxicity. Third, most systems

report liposome rupture while intact liposome adsorption is desirable for controlled release applications. Finally, it is unclear how liposomes interact with GO, reduced GO (rGO) and pristine graphene; the latter two are much more hydrophobic and are likely to involve different intermolecular forces. In this work, all these questions have been answered and we demonstrate stable liposome adsorption by GO without rupturing, while liposome adsorption by rGO or graphene is followed by its rupture. Based on our understanding, light induced liposome content release was realized.

Our liposomes were prepared by the standard extrusion method and dynamic light scattering indicated their average hydrodynamic sizes to be ~110 nm (Figure S2, Supporting Information). To track liposomes using fluorescence, 1% rhodamine (Rh)-modified lipid was included. We first tested the effect of liposome charge by respectively mixing zwitterionic DOPC, anionic DOPG and cationic DOTAP with GO in buffer (10 mM HEPES, pH 7.6, 100 mM NaCl). After centrifugation to precipitate GO, the fluorescence of the samples was observed under UV light in a dark room. The supernatant fluorescence completely disappeared in the presence of GO for both DOPC and DOTAP (Figure 1A and Figure S3 for color). Since our speed of centrifugation (7000 rpm) cannot precipitate free liposomes, the loss of supernatant fluorescence can only be explained by GO adsorption and co-precipitation. As GO is a fluorescence quencher and it forms a dense pellet after centrifugation, the fluorescence of the precipitated liposomes is also masked. The supernatant of anionic DOPG remained highly fluorescent as it was repelled by the negatively charged GO.

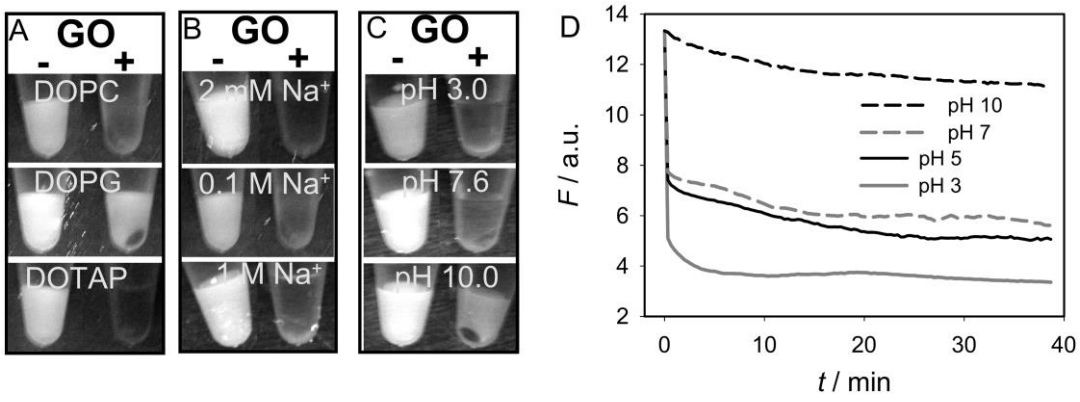

Figure 1. Photographs of Rh-labeled liposomes after mixing with GO and centrifugation as a function of liposome charge (A), salt concentration for DOPC (B) or pH for DOPC (C). Fluorescence change of Rh-labeled DOPC after mixing with GO as a function of pH (E). The salt-dependent studies were performed with 5 mM HEPES buffer (pH 7.6). DOPC=1,2-dioleoyl-sn-glycero-3-phosphocholine, DPPC=1,2-dipalmitoyl-sn-glycero -3-phospho choline, DOTAP=1,2-dioleoyl-3-trimethyl ammonium-propane. See Figure S3 for the colored version.

While adsorption of cationic DOTAP can be easily explained by electrostatic attraction, adsorption of zwitterionic DOPC deserves further studies since an appropriate intermolecular force responsible for this adsorption is not obvious. From the application standpoint, PC lipids are commonly used as biocompatible drug carriers, while cationic DOTAP has high toxicity. We first probed this adsorption reaction as a function of salt concentration and all the samples contained 5 mM HEPES buffer (pH 7.6). Interestingly, effective DOPC adsorption was observed with either just ~2 mM Na^+ (from the HEPES buffer) or with 1 M Na^+ (Figure 1B), indicating that the attractive force takes place under a wide range of ionic strength conditions. The free DOPC liposomes remained stably dispersed under all the tested salt concentrations after centrifugation (e.g. the tubes on the left side of Figure 1B showed homogenous fluorescence), supporting that the observed fluorescence quenching with GO must be due to liposome adsorption. Since a high concentration of salt

can screen the charge interaction, this experiment also suggests that electrostatic interaction might not be the main attractive force. This is understandable since DOPC is overall non-charged (zeta-potential = -2.3 mV in 5 mM HEPES) and GO is negatively charged.

Next we tested the effect of pH. The negative charges on GO are from ionized carboxyl groups, and GO is always negatively charged even at very acidic pH.[27] Adjusting pH changes the fraction of protonated carboxyl. As shown in Figure 1C, retarded DOPC adsorption was observed only at high pH, where more carboxyl groups were deprotonated. Since liposome adsorption by GO is accompanied with fluorescence quenching, we used fluorescence to follow the adsorption kinetics (Figure 1D). Barely any adsorption took place at pH 10. As opposed to the complete quenching shown in Figure 1A, a high fluorescence signal remained in Figure 1D (e.g. fluorescence did not decay to zero). This can be attributed to that adsorption by GO alone cannot completely quench the fluorescence since not all the Rh-labeled lipids are in close proximity to GO (Figure S4).[28] Only after centrifugation, liposomes co-precipitate with GO into a pellet, leaving no fluorescence in the supernatant. From pH 3 to 10, the charging state of DOPC remains unchanged. GO is also negatively charged in this range. Therefore, electrostatic attraction is unlike to take place as abovementioned. We attribute the weakened interaction at high pH to the break of more specific chemical interactions such as hydrogen bonding between the carboxyl on GO and the lipid head group (e.g. the phosphate oxygen).

Next, we probed the effect of hydrophobic interactions using rGO and graphene. rGO was prepared using $NaBH_4$ as a reducing agent.[29] The color of GO changed from yellow to black indicating the formation of more pristine graphene regions (inset of Figure S5D). UV-vis spectrum of rGO showed the elimination of the 300 nm peak, confirming good reduction efficiency (Figure S6). The GO, rGO, and graphene samples used in this work were also characterized by Raman spectroscopy and XPS (Figure S7). The oxygen content of our GO

sample was ~40.8% according to the vendor. After $NaBH_4$ treatment, the oxygen content is dropped to 13.4% based on XPS measurement,[29] while our graphene sample has an oxygen content of less than 2% (note: graphene was prepared by thermal exfoliation reduction plus hydrogen reduction). Our rGO samples could be stably dispersed in water for many days but graphene was easily aggregated in water. We mixed a fixed amount of Rh-labeled DOPC with various concentrations of GO, rGO, or graphene. After centrifugation, both GO and rGO were able to attract liposomes in a concentration-dependent manner and rGO appeared to be even more effective (Figure 2A, B, see Figure S5 for color pictures). This could be related to that rGO has a higher quenching efficiency compared to GO.[30] Adsorption by graphene was much less effective (Figure 2C). To quantify the result and eliminate the difference in quenching efficiency, the supernatant fluorescence representing non-adsorbed free liposomes was measured (Figure 2D) and rGO attracted slightly more DOPC than GO. Our data showed that graphene can still adsorb liposomes. However, since graphene cannot be stably dispersed in water and tends to aggregate, it may reduce its surface area and decrease the adsorption capacity.

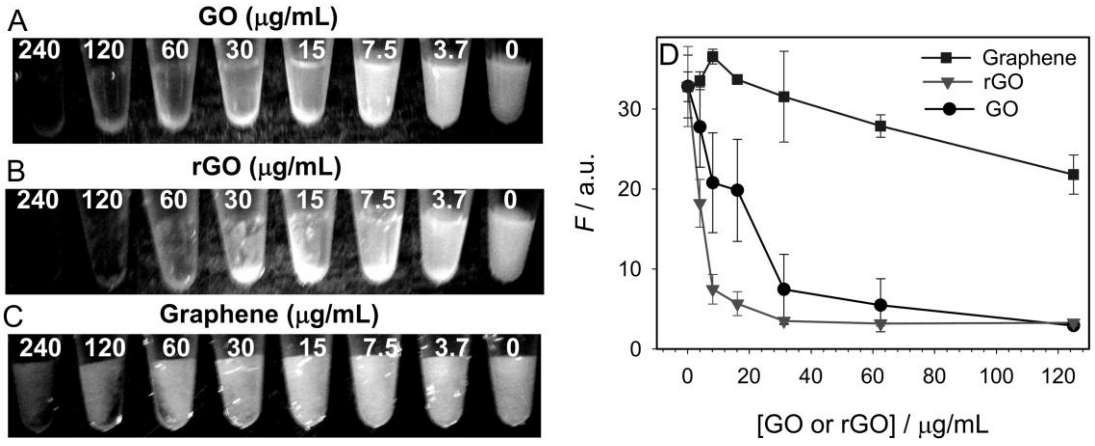

Figure 2. Photograph of various concentrations of GO (A), rGO (B), or graphene (C) mixed with a fixed concentration of Rh-labeled DOPC after centrifugation under 245 nm UV light. (D) The supernatant fluorescence indicating free DOPC after mixing DOPC with GO, rGO, or graphene and centrifugation. See Figure S5 for the colored version.

The above assays confirmed the association of DOPC with GO, rGO, and graphene, and we called it adsorption or attraction. However, liposome adsorption might lead to fusion/rupture and formation of supported bilayers or other structures. To fully test this, we performed cryo-TEM studies on the samples. To achieve a high liposome loading, the sample was prepared with an excess of DOPC liposomes. As shown in Figure 3A, intact liposomes are still observed on the GO surface. Therefore, at least a portion of the adsorbed liposomes are not ruptured. Figure 3A shows that liposomes are only sparsely distributed on the GO sheet, even though we used an excess amount of the liposome. Therefore, there are specific regions with higher adsorption affinity while other regions cannot stably adsorb the liposome. In particular, most of the liposomes were associated with the edges of the GO sheets, which are highly oxidized and rich in carboxyl groups.[31-36] This is also in line with the above pH-dependent study. Extensive bridging can lead to aggregation (Figure 3B), where many deformed liposomes are observed. Based on this cryo-TEM work alone, we conclude that at least a fraction of liposomes are adsorbed by GO and do not undergo fusion/rupture.

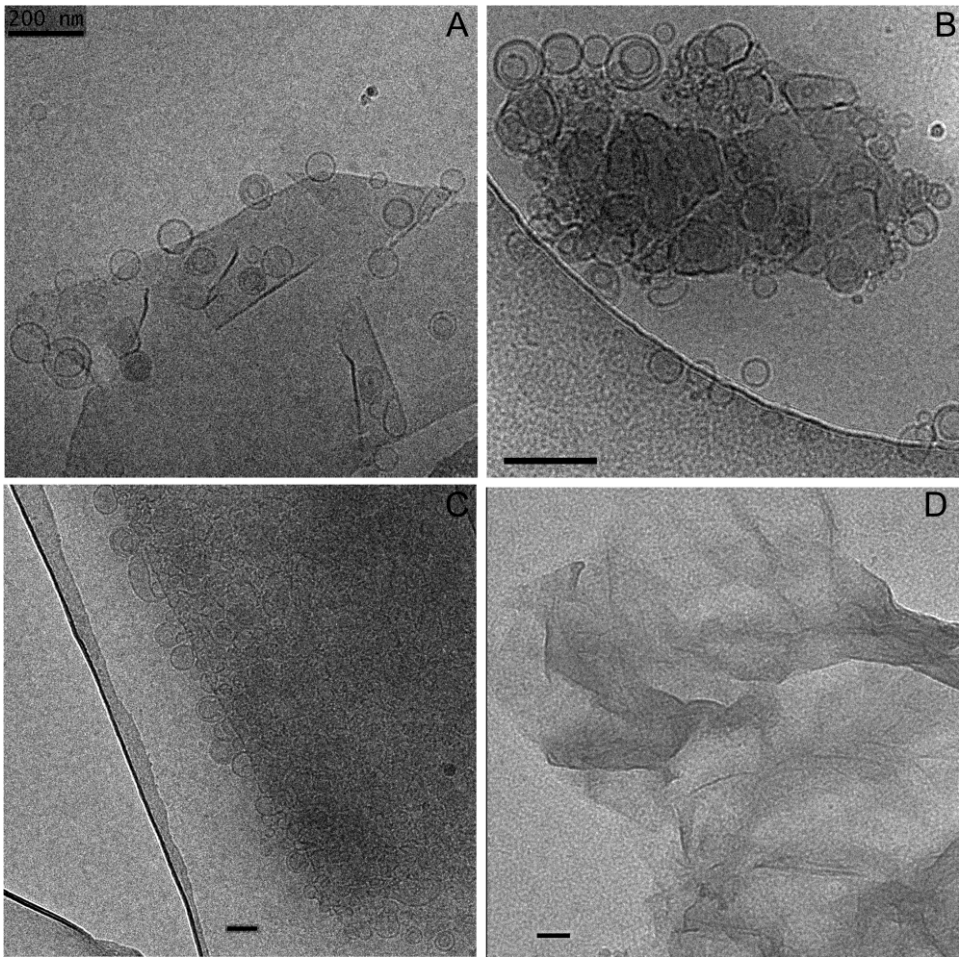

Figure 3. Cryo-TEM micrographs of the DOPC/GO mixture (A, B), DOPC/rGO (C), and DOPC/graphene (D). In all the samples DOPC was used in excess to promote possible fusion and non-associated liposomes were washed away before imaging. (A) DOPC distributes sparsely on the edge of a GO sheet. (B) An aggregated structure. (C) DOPC is very densely adsorbed by rGO. (D) Barely any intact liposomes could be found on the graphene sample. Scale bar = 200 nm in (A, B) and 100 nm in (C, D).

As shown in Figure 3C, rGO adsorbs a very high density of DOPC. The liposome coverage was so high that only the edge the sample could be resolved. This is consistent with its high liposome loading capacity shown in Figure 2 based on fluorescence measurement. On the other hand, barely any intact liposomes could be found for the graphene sample (Figure 3D). This may suggest that the majority of the adsorbed liposomes were ruptured on graphene.

Based on the TEM data alone, however, it is difficult to test liposome fusion/rupture. For example, ruptured liposomes are likely to form supported lipid layers on GO, which may not have the appropriate contrast to be imaged by TEM. There is also no information on whether the content inside the adsorbed liposomes leaks or not. To further understand this, we encapsulated a high concentration of calcein into DPPC so that the fluorescence inside the liposome was self-quenched. DPPC was chosen because it has a phase transition temperature (T_c) of 41 °C, which is useful for designing controlled release materials. For comparison, T_c of DOPC is -20 °C, disallowing temperature-controlled release. If liposomes rupture on GO, an increase of fluorescence should occur due to release of calcein into solution. The fluorescence of calcein encapsulated DPPC was very stable at room temperature and no change was observed in 20 min (Figure 4A, solid black curve). At this time point, Triton X-100 was added to completely rupture the liposome so that the percentage of calcein release can be quantified. This sample serves as a negative control to show that calcein does not leak out spontaneously at room temperature. Next, DPPC and GO were mixed at high concentration to promote adsorption and this mixture was diluted in buffer. We confirmed that >95% of the liposomes were adsorbed by GO by measuring the supernatant fluorescence after centrifugation (Figure S9). Note that the DPPC liposomes used here were not labeled with Rh and this also served as a control to show the Rh label is not required for liposome adsorption. In this case, little fluorescence change was observed either (Figure 4A, gray dashed curve), supporting the lack of fusion/rupture/leakage of DPPC upon adsorption by GO. The presence of intact liposomes suggests the possibility of using GO/liposome conjugates for controlled release applications.

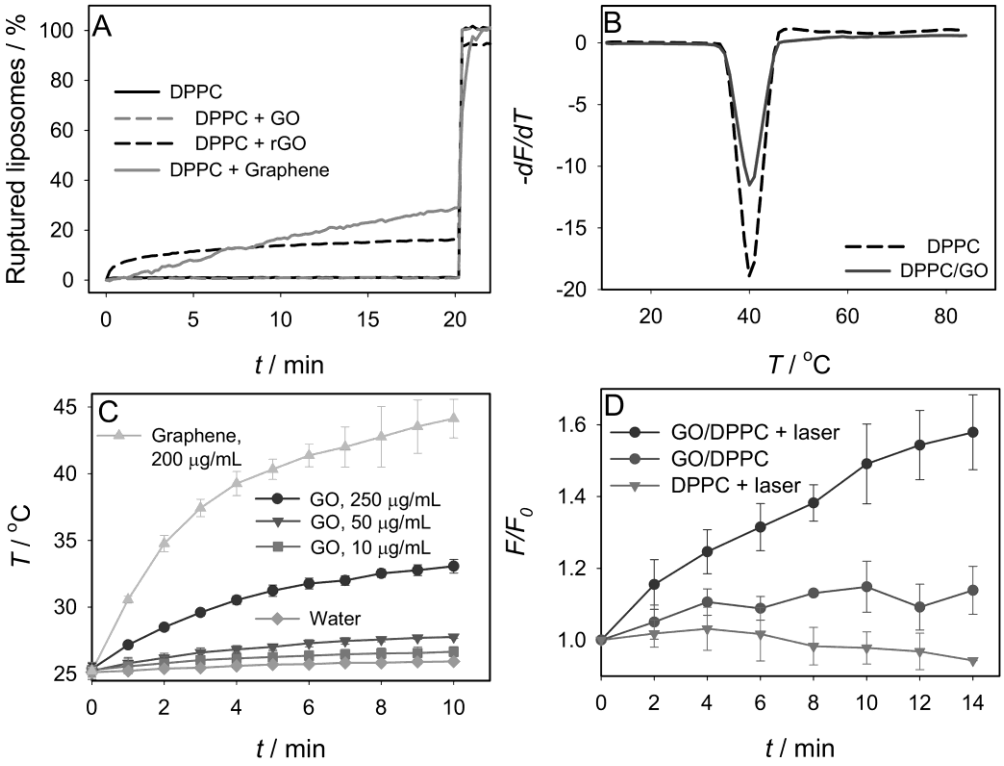

Figure 4. (A) Kinetics of fluorescence increase indicating liposome rupture after mixing calcein loaded DPPC with GO, rGO, or graphene. Triton was added at 20 min. (B) Calcein release from DPPC as a function of temperature. (C) Water heating by a 808 nm laser with various concentrations of GO or graphene. (D) Calcein leakage from DPPC induced by a 808 nm laser in the presence or absence of GO.

Interestingly, when DPPC was mixed with rGO, fluorescence increase was observed, indicating rupture of the liposome (Figure 4A, black dashed curve). The majority of the liposomes were adsorbed by rGO right after mixing. Liposome rupture, on the other hand, took a longer time, suggesting that the kinetics of liposome rupture is much slower than adsorption. In other words, the rupture activation energy barrier is higher than the adsorption energy barrier. Retarded calcein release at a lower temperature of 10 °C further confirmed that thermal energy is required for liposome to rupture on rGO (Figure S11).

We noticed that not all adsorbed DPPC was ruptured by rGO since Triton still induced a significant fluorescence increase. In fact, only ~18% of the added DPPC ruptured in 20 min

based on Figure 4A. The percentage of ruptured liposomes did not increase much with an even longer incubation time of 23 hr (Figure S12A) or using more rGO (Figure S12B). It is known that for rGO prepared by $NaBH_4$ reduction, the carboxyl on the edge of remains.[37] Therefore, liposomes adsorbed on these positions are likely to remain intact, explaining the incomplete rupture. The cryo-TEM data in Figure 3C also supports the presence of intact liposomes on rGO. Following the trend of reducing oxygen level, it is thus interesting to test graphene. From Figure 2 we know that the liposome adsorption capacity is much lower for graphene. To achieve a clean background, we centrifuged the DPPC/graphene mixture and removed the free liposomes. In this case, we observed ~30% calcein release in 20 min and ~70% release was achieved in 3 h (Figure S13). Since our graphene sample still contained ~2% oxygen, it is likely that complete rupture can be realized given enough time with real pristine graphene. We have repeated the leakage experiments also with calcein loaded DOPC liposomes and similar results were obtained (Figure S14). It appears that DOPC leaks more easily since rGO induced ~50% DOPC leakage as compared to ~18% for DPPC.

The nanoscale structures of GO, rGO, and graphene have been carefully characterized. For example, GO is mostly amorphous because of sp^3 C-O bonds and the oxygen content can reach a very high value (e.g. carbon:oxygen = 1.67 for our GO sample).[36] Carboxyl groups are often distributed on the edges.[34] rGO contains both hydrophilic highly oxidized domains and crystalline hydrophobic carbon domains; the size of both domains is on the scale of 5-8 nm.[32] Graphene is mostly crystalline carbon.[38] Our cryo-TEM micrographs indicate that liposomes are only sparsely distributed on GO, with the highest occurrence along the edges. Considering that low pH is required for DOPC adsorption, we reason that the liposomes might sit on the oxidized hydrophilic regions (*e.g.* the edges) to interact with GO via hydrogen bonding and van der Waals force. A possible hydrogen bonding interaction is between the carboxyl and the phosphate oxygen in the PC lipid. The non-electrostatic nature

of GO/PC interaction might be employed to engineer new hybrid materials that are insensitive to salt concentration. Intact liposomes can be accommodated in the small domains of GO, but to initiate liposome rupture, a certain pristine graphene domain size is likely to be required, explaining the incomplete rupture on rGO. For graphene, the initial adsorption is difficult to take place in the colloidal conditions, but the adsorbed liposomes are almost completely ruptured. Therefore, rGO has an interesting combination of hydrophilicity and hydrophobicity in the nanodomain format, allowing both effective adsorption and subsequent rupture.

After knowing that DPPC adsorbs by GO as intact liposomes, we aim to test whether controlled content release could be achieved taking advantage that GO may convert radiation into heat. We first dispersed various concentrations of GO in water and the water temperature was increased using a near IR 808 nm laser in a GO concentration dependent manner (Figure 4C). For example, the temperature of 250 μg mL^{-1} GO was increased by ~6 °C in 10 min while graphene induced ~20 °C increase. This experiment confirms the conversion of laser light into thermal energy. Similar effects were also observed with carbon nanotubes and various graphene-based materials.[39, 40] To avoid heating of the bulk water, we used a final GO concentration of 0.9 μg mL^{-1}, at which the water temperature barely changed.

We next tested thermally induced calcein leakage from DPPC. The fluorescence of both calcein loaded free DPPC and DPPC adsorbed by GO was monitored as a function of temperature. The first derivative of fluorescence change is shown in Figure 4B; both samples showed almost no release at below 30 °C or above 50 °C; the fastest release occurred at around 40 °C, which is close to the T_c of DPPC. This experiment indicating that adsorption by GO did not disrupt the phase transition behavior of DPPC. In addition, if the local heating can reach ~40 °C nearby the liposome, fast content release can then be achieved.

To test light controlled release, calcein loaded DPPC was mixed with GO. We exposed the GO/DPPC mixture to the 808 nm laser and measured fluorescence at 2 min

intervals. As shown in Figure 4D, >50% fluorescence enhancement was achieved after 14 min. Without laser, the change was ~10%. If no GO was added, exposing DPPC alone to laser did not cause much fluorescence change either. Therefore, we achieved near IR light-induced liposome content release. Since this wavelength is largely transparent to the human tissue, this might be useful for controlled release and therapy *in vivo*.

We have summarized our main findings in Figure 5. Non-electrostatic interactions can be harnessed to adsorb liposomes. Zwitterionic PC liposomes interact with GO, rGO and graphene via different mechanisms. GO relies on a pH-dependent force and liposomes are stably adsorbed on the edges of GO. On the other hand, rGO and graphene induce liposome rupture following the adsorption step. The fraction of liposome undergoing rupture is a function of the level of oxidation. These understandings are important for designing of biomaterials based on graphene to interface with cells and may shine light on the cytotoxicity of graphene-based materials. From the fundamental aspect, this study also reveals intriguing intermolecular forces that direct totally different interactions with liposomes based on the surface chemistry of graphene.

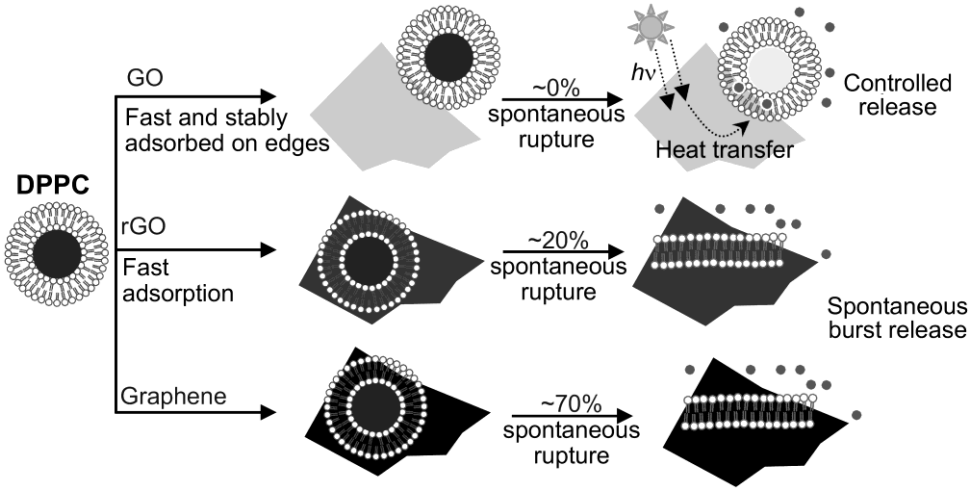

Figure 5. Schematics of PC liposomes interacting with GO, rGO and graphene. For light induced content release, DPPC or other high T_c lipids are required.

Experimental Section

Chemicals. All the phospholipids were purchased from Avanti Polar Lipids (Alabaster, AL). GO and graphene were purchased from ACS Material, LLC **(**Medford, MA). Disodium calcein was purchased from Sigma-Aldrich. 2-(N-morpholino)ethanesulfonic acid (MES), 4-(2-hydroxyethyl)-1-piperazineethanesulfonic acid (HEPES), trisodium citrate, NaOH, sodium phosphate and NaCl were purchased from Mandel Scientific (Guelph, ON, Canada). Mill-Q water was used to prepare all the buffers and solution.

Preparation of rGO. The procedures for preparing liposomes are presented in Supporting Information. To minimize the change of graphene concentration during the reduction reaction, dispersed GO solution was directly added to $NaBH_4$ powder to achieve a final $NaBH_4$ concentration of 150 mM. The reduction was carried out at ~50 °C for 20 min (leave the cap open) followed by incubating at room temperature for 1 day. The color of the sample turned black while colloidal stability can be maintained for more than a week.

Visual observation of liposome adsorption: In a typical experiment, GO (50 μL, 0.26 mg mL^{-1}) with designated salt or pH was mixed with Rh-labeled liposome (1 μL, 2.5 mg mL^{-1}). After 5 min incubation, the sample was centrifuged (7000 rpm, 10 min) before it was observed in a dark room under the excitation of a handheld UV lamp (245 nm). The pictures were taken using a digital camera. pH was adjusted with phosphate buffers (25 mM, pH 3, 5, 7), or HEPES buffer (pH 7.6). NaOH was used to adjust pH to 10. Similar procedures were used to observe liposome adsorption by rGO and by graphene. To quantify the non-adsorbed free liposome, the supernatant solution after centrifugation (2 μL) was transferred to MES buffer (100 μL, 20 mM, pH 6.0) and the fluorescence intensity was read by a fluorescence microplate reader (Infinite Pro F200, Tecan) using the rhodamine channel.

Adsorption kinetics: The liposome adsorption kinetics was monitored using the fluorescence microplate reader (100 μL for each sample, final GO concentration = 130 μg mL^{-1} and the

final Rh-labeled DOPC = 25 μg mL^{-1}). The fluorescence of the same samples but without GO was also monitored as reference.

Cryo-TEM: GO (40 μL, 200 μg mL^{-1}) was mixed with DOPC (80 μL, 2.5 mg mL^{-1}) in buffer at 60 °C for 30 min. The excess amount of liposome was removed after centrifugation. TEM samples were prepared by spotting the liposome suspension (5 μL) on a carbon coated copper TEM grid (treated with plasma to ensure surface was hydrophilic) in a humidity controlled chamber (FEI Vitrobot). The humidity was set to be 95 to 100% during this operation. The grid was blotted with two filter papers for 1.5 sec and quickly plunged into liquid ethane. The sample was then loaded to a liquid N_2 cooled cold stage and loaded into a 200 kV field emission TEM (FEI Tecnai G2 F20). The samples were imaged when the temperature was stabilized at -175 °C. Samples containing rGO and graphene were incubated at room temperature and other procedures remained the same.

Calcein release assays. The above purified calcein loaded DPPC was used to monitor liposome rupture. In a typical experiment, DPPC liposome (10 μL) was mixed with GO (10 μL, 260 μg mL^{-1}) or rGO and the mixture was quickly transferred to MES (1.5 mL, 20 mM, pH 6.0) in a quartz cuvette. The fluorescence was monitored every 12 sec for 20 min before Triton X-100 (10 μL, 5%) was added to fully rupture the liposomes and the fluorescence was read again. To test the effect of temperature, the cuvette was cooled to 10 °C before the liposome/rGO mixture was added.

For calcein releasing from DPPC/graphene, DPPC (25 μL) and graphene (50 μL, 260 μg mL^{-1}) was mixed for 30 sec and the sample was centrifuged at 7000 rpm for 2 min. The supernatant was gently removed and the precipitant was washed twice with MES buffer (100 μL each time). Some graphene might be lost during this process since they tend to float on water. After washing, the sample was transferred to the cuvette containing MES buffer (pH

6.0, 20 mM) and the fluorescence was monitored over a designated period of time before Triton X-100 was added.

Laser heating water in the presence of GO or graphene. In a 1cm × 1cm fluorescence quartz cuvette, 1.5 mL sample with various concentration of GO or graphene was added. The 808 nm laser (1 W, diode laser) was placed ~ 5 cm from the cuvette and the temperature of water was measured using a thermal couple every min. The experiments were run in triplicate.

Laser induced calcein release from DPPC/GO. In each experiment, GO (10 μL, 260 μg mL^{-1}) was mixed with 20 μL calcein loaded DPPC and 14 μL of the mixture was transferred to each cuvette containing 1.5 mL buffer (20 mM MES, pH 6.0). One cuvette was exposed to the 808 nm laser at a distance of ~5 cm and the other cuvette was placed next to it without exposure to the laser. Fluorescence was measured every 2 min in the cuvette port of a SpectraMax M3 plate reader. The experiments were run in triplicate. The effect of laser exposure on free DPPC liposome was also measured for comparison, where 10 μL of the buffer was mixed with 20 μL of the liposome and the other operations were the same.

Acknowledgements

We thank Dr. Liyan Zhao for assistance for Raman and XPS spectroscopy. Funding for this work is from the University of Waterloo, the Canadian Foundation for Innovation, and the Natural Sciences and Engineering Research Council (NSERC) of Canada and the Early Researcher Award from the Ontario Ministry of Research and Innovation.

References

[1] A. K. Geim, K. S. Novoselov, *Nat. Mater.* **2007**, *6*, 183.

[2] M. J. Allen, V. C. Tung, R. B. Kaner, *Chem. Rev.* **2009**, *110*, 132.

[3] C. N. R. Rao, A. K. Sood, K. S. Subrahmanyam, A. Govindaraj, *Angew. Chem. Int. Ed.* **2009**, *48*, 7752.

[4] K. P. Loh, Q. Bao, G. Eda, M. Chhowalla, *Nat Chem* **2010**, *2*, 1015.

[5] Y. W. Zhu, S. Murali, W. W. Cai, X. S. Li, J. W. Suk, J. R. Potts, R. S. Ruoff, *Adv. Mater.* **2010**, *22*, 3906.

[6] Y. Wang, Z. H. Li, J. Wang, J. H. Li, Y. H. Lin, *Trends Biotechnol.* **2011**, *29*, 205.

[7] J. Kim, L. J. Cote, J. Huang, *Acc. Chem. Res.* **2012**, *45*, 1356.

[8] X. M. Sun, Z. Liu, K. Welsher, J. T. Robinson, A. Goodwin, S. Zaric, H. J. Dai, *Nano Research* **2008**, *1*, 203.

[9] Z. Liu, J. T. Robinson, X. M. Sun, H. J. Dai, *J. Am. Chem. Soc.* **2008**, *130*, 10876.

[10] K. Yang, S. A. Zhang, G. X. Zhang, X. M. Sun, S. T. Lee, Z. A. Liu, *Nano Lett.* **2010**, *10*, 3318.

[11] Y. Wang, Z. H. Li, D. H. Hu, C. T. Lin, J. H. Li, Y. H. Lin, *J. Am. Chem. Soc.* **2010**, *132*, 9274.

[12] S. J. He, B. Song, D. Li, C. F. Zhu, W. P. Qi, Y. Q. Wen, L. H. Wang, S. P. Song, H. P. Fang, C. H. Fan, *Adv. Funct. Mater.* **2010**, *20*, 453.

[13] C. H. Lu, H. H. Yang, C. L. Zhu, X. Chen, G. N. Chen, *Angew. Chem. Int. Ed.* **2009**, *48*, 4785.

[14] X. H. Zhao, R. M. Kong, X. B. Zhang, H. M. Meng, W. N. Liu, W. H. Tan, G. L. Shen, R. Q. Yu, *Anal. Chem.* **2011**, *83*, 5062.

[15] H. X. Chang, L. H. Tang, Y. Wang, J. H. Jiang, J. H. Li, *Anal. Chem.* **2010**, *82*, 2341.

[16] C. Peng, W. B. Hu, Y. T. Zhou, C. H. Fan, Q. Huang, *Small* **2010**, *6*, 1686.

[17] R. Kempaiah, A. Chung, V. Maheshwari, *ACS Nano* **2011**, *5*, 6025.

[18] P. K. Ang, M. Jaiswal, C. H. Y. X. Lim, Y. Wang, J. Sankaran, A. Li, C. T. Lim, T. Wohland, O. Barbaros, K. P. Loh, *ACS Nano* **2010**, *4*, 7387.

[19] R. Frost, G. E. Jonsson, D. Chakarov, S. Svedhem, B. Kasemo, *Nano Lett.* **2012**, *12*, 3356.

[20] A. V. Titov, P. Kral, R. Pearson, *ACS Nano* **2009**, *4*, 229.

[21] Y. Okamoto, K. Tsuzuki, S. Iwasa, R. Ishikawa, A. Sandhu, R. Tero, in *Asia-Pacific Interdisciplinary Research Conference 2011*, Vol. 352 (Ed: A. Sandhu), Iop Publishing Ltd, Bristol **2012**, 012017.

[22] K. Tsuzuki, Y. Okamoto, S. Iwasa, R. Ishikawa, A. Sandhu, R. Tero, in *Asia-Pacific Interdisciplinary Research Conference 2011*, Vol. 352 (Ed: A. Sandhu), Iop Publishing Ltd, Bristol **2012**, 012016.

[23] E. Sackmann, *Science* **1996**, *271*, 43.

[24] B. Wang, L. F. Zhang, S. C. Bae, S. Granick, *Proc. Natl. Acad. Sci. U.S.A.* **2008**, *105*, 18171.

[25] H. J. Liang, D. Harries, G. C. L. Wong, *Proc. Natl. Acad. Sci. U.S.A.* **2005**, *102*, 11173.

[26] A. M. Smith, M. Vinchurkar, N. Gronbech-Jensen, A. N. Parikh, *J. Am. Chem. Soc.* **2010**, *132*, 9320.

[27] L. J. Cote, J. Kim, Z. Zhang, C. Sun, J. X. Huang, *Soft Matter* **2010**, *6*, 6096.

[28] P.-J. J. Huang, J. Liu, *Small* **2012**, *8*, 977.

[29] H.-J. Shin, K. K. Kim, A. Benayad, S.-M. Yoon, H. K. Park, I.-S. Jung, M. H. Jin, H.-K. Jeong, J. M. Kim, J.-Y. Choi, Y. H. Lee, *Adv. Funct. Mater.* **2009**, *19*, 1987.

[30] J. Kim, L. J. Cote, F. Kim, J. Huang, *J. Am. Chem. Soc.* **2010**, *132*, 260.

[31] T. Szabo, O. Berkesi, P. Forgo, K. Josepovits, Y. Sanakis, D. Petridis, I. Dekany, *Chem. Mater.* **2006**, *18*, 2740.

[32] C. Gomez-Navarro, J. C. Meyer, R. S. Sundaram, A. Chuvilin, S. Kurasch, M. Burghard, K. Kern, U. Kaiser, *Nano Lett.* **2010**, *10*, 1144.

[33] W. Cai, R. D. Piner, F. J. Stadermann, S. Park, M. A. Shaibat, Y. Ishii, D. Yang, A. Velamakanni, S. J. An, M. Stoller, J. An, D. Chen, R. S. Ruoff, *Science* **2008**, *321*, 1815.

[34] A. Lerf, H. He, M. Forster, J. Klinowski, *J. Phys. Chem. B* **1998**, *102*, 4477.

[35] K. N. Kudin, B. Ozbas, H. C. Schniepp, R. K. Prud'homme, I. A. Aksay, R. Car, *Nano Lett.* **2007**, *8*, 36.

[36] K. A. Mkhoyan, A. W. Contryman, J. Silcox, D. A. Stewart, G. Eda, C. Mattevi, S. Miller, M. Chhowalla, *Nano Lett.* **2009**, *9*, 1058.

[37] W. Gao, L. B. Alemany, L. Ci, P. M. Ajayan, *Nat Chem* **2009**, *1*, 403.

[38] M. Ishigami, J. H. Chen, W. G. Cullen, M. S. Fuhrer, E. D. Williams, *Nano Lett.* **2007**, *7*, 1643.

[39] N. W. S. Kam, M. O'Connell, J. A. Wisdom, H. J. Dai, *Proc. Natl. Acad. Sci. U.S.A.* **2005**, *102*, 11600.

[40] J. T. Robinson, S. M. Tabakman, Y. Liang, H. Wang, H. Sanchez Casalongue, D. Vinh, H. Dai, *J. Am. Chem. Soc.* **2011**, *133*, 6825.